

Dielectric Control of Counterion-Induced Single-Chain Folding Transition of DNA

Damien Baigl and Kenichi Yoshikawa

Department of Physics, Graduate School of Science, Kyoto University, Kyoto 606-8502, Japan

ABSTRACT In the presence of condensing agents, single chains of giant double-stranded DNA undergo a first-order phase transition between an elongated coil state and a folded compact state. To connect this like-charged attraction phenomenon to counterion condensation, we performed a series of single-chain experiments on aqueous solutions of DNA, where we varied the extent of counterion condensation by varying the relative dielectric constant ϵ_r from 80 to 170. Single-chain observations of changes in the conformation of giant DNA were performed by transmission electron microscopy and fluorescence microscopy, with tetravalent spermine (SPM⁴⁺) as a condensing agent. At a fixed dielectric constant, single DNA chains fold into a compact state upon the addition of spermine, whereas at a constant spermine concentration single DNA chains unfold with an increase in ϵ_r . In both cases, the transition is largely discrete at the level of single chains. We found that the critical concentration of spermine necessary to induce the single-chain folding transition increases exponentially as the dielectric constant increases, corresponding to 87–88% of the DNA charge neutralized at the onset of the transition. We also observed that the toroidal morphology of compact DNA partially unfolds when ϵ_r is increased.

INTRODUCTION

DNA is a semiflexible highly charged polyelectrolyte that assumes an elongated coil conformation in water. Conversely, in cells, millimeter- to meter-long genomic DNA is usually folded into a dense and compact state to fit within 10^{-4} – 10^{-6} times smaller spaces, such as in the nucleus of eukaryotic cells or viral capsids. This remarkable compaction can be reproduced *in vitro* by adding a small amount of condensing agent (Bloomfield, 1996), such as polyamines (Gosule and Schellman, 1976), multivalent metal cations (Widom and Baldwin, 1983), cationic surfactants (Mel'nikov et al., 1995), or neutral polymers to a DNA solution (Laemmli, 1975). In fact, the folding transition between the elongated coil state and the compact state is largely discrete at the level of single chains and can be described as a first-order phase transition (Yoshikawa et al., 1996). The attractive force between negatively charged monomers is an example of a more general phenomenon called like-charged attraction, which is responsible for various types of macromolecular organization in charged systems, such as bundling and cross-linking of F-actin (Tang and Janmey, 1996; Wong et al., 2003), precipitation of flexible polyelectrolytes (Olvera de la Cruz et al., 1995) and clustering in colloidal suspensions (Grier, 2003). Since the pioneering interpretation by Oosawa (1971), like-charged attraction has been the subject of many theoretical works (Borukhov et al., 2001; Ha and Liu, 1997; Rouzina and Bloomfield, 1996; Shklovskii, 1999; Desemo et al., 2003) and numerical simulations (Grønbech-Jensen et al., 1997; Lyubartsev et al., 1998; Stevens, 1999), which all show, despite

fundamental discrepancies, the crucial role of counterions, especially those that are localized in the vicinity of the charged chain and usually referred to as “condensed” (in fact, counterions are continuously distributed around the chain, as shown recently by anomalous x-ray scattering; Das et al., 2003). However, the like-charged attraction phenomenon has not been unambiguously clarified yet, probably due to the paucity of precise experiments on model systems with a variable number of condensed counterions. Furthermore, many previous studies on charged polyelectrolytes have not distinguished between the single-chain phenomenon (e.g., DNA compaction) and multiple-chain aggregation. To obtain fundamental knowledge on like-charged attraction in a single polyelectrolyte chain induced by counterion condensation, we studied the folding transition of single DNA chains under various dielectric fields.

In the so-called Manning-Oosawa condensation theory (Manning, 1969; Oosawa, 1971), a fraction θ of counterions “condense” on the chain when the average spacing b between charges along the chain becomes smaller than the Bjerrum length l_B , the distance at which the electrostatic energy equals $k_B T$:

$$l_B = \frac{e^2}{4\pi\epsilon_0\epsilon_r k_B T}, \quad (1)$$

where e is the elementary charge, ϵ_0 is the dielectric constant of vacuum, ϵ_r is the relative dielectric constant, k_B is the Boltzmann constant, and T is the temperature. Counterions condense so that the effective distance between charges equals l_B . Thus, for counterions of valency Z , we have

$$\theta = 1 - \frac{b}{Zl_B}. \quad (2)$$

Submitted January 12, 2005, and accepted for publication February 22, 2005.

Address reprint request to Kenichi Yoshikawa, Tel.: 81-75-753-3812; Fax: 81-75-753-3779; E-mail: yoshikaw@scphys.kyoto-u.ac.jp.

© 2005 by the Biophysical Society

0006-3495/05/05/3486/08 \$2.00

doi: 10.1529/biophysj.105.059493

For DNA in pure water at 20°C, $b = 0.17$ nm, $l_B = 0.71$ nm, and $\theta = 0.76$ in the case of monovalent counterions. Therefore, θ can be decreased by decreasing l_B or increasing ϵ_r at constant temperature. For instance, the Bjerrum length of a solvent such as *N*-methylformamide can be decreased with temperature, from 0.45 nm at 70°C to 0.30 nm at 10°C (Bass et al., 1964; Sehgal and Seery, 1998). In this study, the dielectric constant of water at room temperature was enhanced by the dissolution of zwitterionic species, with ϵ_r ranging from 80 to 170, l_B from 0.71 to 0.33 at 20°C, and θ from 76% to 48% (in the case of sole monovalent counterions). The condensation of DNA in the presence of zwitterionic species to achieve a high dielectric constant has been studied in detail by Houssier et al. (Flock et al., 1995, 1996; Flock and Houssier, 1997). However, in these pioneering experiments, DNA concentration was quite large; i.e., the phenomenon was observed in the ensemble of a large number of chains where the single-chain compaction can not be studied due to the effect of multichain precipitation. To our knowledge, we report here the first experimental study on the folding transition of single double-stranded DNA molecules as a function of an increasing dielectric constant. Direct single-chain observation in bulk was performed by fluorescence microscopy, and transmission electron microscopy was used to study the detailed morphology of the compact states. The results have enabled us to establish the phase diagram of single-chain conformation as a function of an increasing dielectric constant, i.e., with a decrease in the extent of counterion condensation.

MATERIALS AND METHODS

Materials

Stock solutions of bacteriophage T4 DNA (166 kbp; Nippon Gene, Tokyo, Japan), were prepared in a 10 mM Tris-HCl buffer solution (pH = 7.4). For zwitterionic species, we used glycine, 4-aminopropanoic acid and 6-aminohexanoic acid (Nacalai Tesque, Kyoto, Japan), which have dielectric increments of 22.6, 51.0, and 77.5 L.mol⁻¹, respectively. They were dissolved at various concentrations to obtain relative dielectric constants ϵ_r ranging from 80 to 170. As a condensing agent, we used spermine tetrahydrochloride (Nacalai Tesque), a tetravalent cationic polyammonium salt, abbreviated SPM⁴⁺.

Fluorescence microscopy

Very dilute DNA solutions were prepared at 0.1 μ M (in nucleotides) with 0.1 μ M of the fluorescent dye 4'6-diamidino-2-phenylindole, abbreviated DAPI (Wako Pure Chemical Industries, Osaka, Japan). Fluorescent microscopic observations were performed using an Axiovert 135 TV (Carl Zeiss, Aalen, Germany) microscope equipped with a 100 \times oil-immersed lens. Images were recorded using an EB-CCD camera and an image processor Argus 10 (Hamamatsu Photonics, Hamamatsu, Japan). Samples were placed in custom-built microscope cells (made of glass previously cleaned by baking at 500°C for 1 h), illuminated at 365 nm, and observed at $\lambda \geq 420$ nm. Due to the blurring effect of fluorescence light, the apparent sizes of fluorescent images are ~ 0.3 μ m larger than the actual sizes (Yoshikawa and Matsuzawa, 1995). Under these experimental conditions, we can directly observe the bulk conformation of a large number of individual DNA chains.

The coil and compact states of individual chains are clearly distinguishable: compared to folded compact DNA, which appears as a bright fast-diffusing spot, DNA in the coil state has a much larger apparent long-axis length (longest distance in the outline of the DNA image), has a much lower translational diffusion coefficient, and exhibits characteristic intra-chain thermal fluctuations.

Transmission electronic microscopy

Transmission electronic microscopic (TEM) observations were performed at room temperature using a JEM-1200EX microscope (JEOL, Tokyo, Japan) at an acceleration voltage of 100 kV and with an H-7000 microscope (Hitachi, Tokyo, Japan) at 75 kV. We used carbon-coated grids with a mesh size of 300 and uranyl acetate (1% in water) as staining agent.

RESULTS

Coil state

First, we studied the effect of increasing ϵ_r on the general properties of individual DNA chains in the absence of spermine. Using fluorescent microscopy, we observed that, for ϵ_r ranging from 80 to 158, all individual chains are in the characteristic elongated coil state. Image analysis has allowed us to measure the long-axis length L of individual DNA molecules. Fig. 1 shows L , averaged for 150 individual molecules, plotted as a function of ϵ_r . Within the limits of our experimental accuracy, L is independent of ϵ_r and equals ~ 4.4 μ m. This value suggests that the persistence length l_p remains essentially constant (~ 50 nm; Yoshinaga et al., 2002) regardless of changes in ϵ_r . In the Odijk or Skolnick and Fixman theories (OSF) for rigid polyelectrolytes in the presence of monovalent salts, l_p is the sum of the bare persistence length l_0 and the electrostatic persistence length $l_{OSF} \approx 1/(4\kappa^2 l_B)$ (Odijk, 1977; Skolnick and Fixman, 1977). κ^{-1} is the Debye length and $\kappa^2 = 8\pi l_B C_s$ where C_s is the total salt concentration. In the conditions of our experiments where 10 mM of monovalent salts come from the buffer solution, we can estimate $l_{OSF} \approx \epsilon_r^2/1953$. Therefore, in the range of ϵ_r investigated here, the variation of l_p is $<25\%$. The corresponding variation in the long-axis length is $\sim 10\%$,

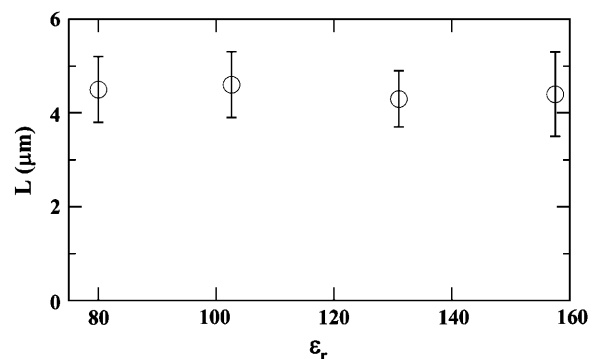


FIGURE 1 Long-axis length L of individual T4 DNA chains (0.1 μ M) as a function of the relative dielectric constant in the absence of spermine (coil state). Each point represents the average of 150 individual molecules.

which cannot be detected within the experimental accuracy of our experiments.

To characterize the effects of ϵ_r on the secondary structure of DNA, circular dichroism (CD) measurements were performed as well. These experiments were performed at a DNA concentration of $15 \mu\text{M}$ (in nucleotides), which under our conditions is the lowest DNA concentration that allows for CD measurement with a reasonable signal to noise ratio. On the other hand, it has been shown that above $10 \mu\text{M}$, T4 DNA chains start to interact (Iwataki et al., 2004). Therefore, strictly speaking, a $15 \mu\text{M}$ DNA solution cannot be considered a dilute solution. However, under our experimental conditions, neither precipitation nor aggregation was observed in the prepared specimen, which indicates that DNA chains interact in a very weak manner. Thus we can assume that the CD spectra obtained under these conditions reflect the CD properties of individual chains. Fig. 2 shows CD spectra for $15 \mu\text{M}$ DNA solutions at various dielectric constants ϵ_r . Within the limits of our experimental accuracy, all curves have a similar shape and present two characteristic bands: negative at $\lambda = 245\text{--}250 \text{ nm}$ and positive at $\lambda = 275\text{--}285 \text{ nm}$. The low DNA concentration results in somewhat larger experimental error compared to usual conditions. Thus, we will not discuss the minor changes observed in the CD spectra. The presence of the two characteristic bands shows that individual DNA chains are in the B-form throughout the entire range of ϵ_r investigated here. The secondary structure, or the spatial arrangement of bases, is thus unaffected by the dielectric constant, which essentially controls the electrostatic interactions. Therefore, in the absence of condensing agents, regardless of ϵ_r within the range $80\text{--}158$, all chains are in an elongated coil state, have a similar characteristic size, and are composed of B-DNA.

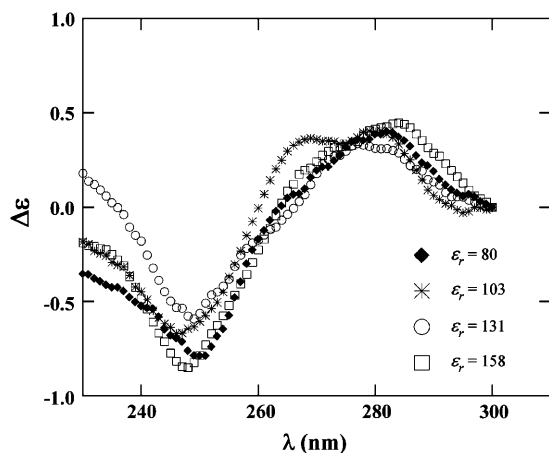


FIGURE 2 CD spectra of DNA ($15 \mu\text{M}$) at various dielectric constants: 80 (\blacklozenge), 103 ($*$), 131 (\circ), and 158 (\square). DNA solutions are in pure water, glycine 1 M, 4-aminopropanoic acid 1M, and 6-aminoheptanoic acid 1M, respectively.

Single-chain folding transition in pure water

Fig. 3 shows the effect of the addition of tetravalent spermine to a dilute solution of DNA in water ($\epsilon_r = 80$). As long as the spermine concentration $[\text{SPM}^{4+}]$ is $< 4.5 \mu\text{M}$, all chains are in the coil state (*a*) and their long-axis length is independent of $[\text{SPM}^{4+}]$. In contrast, for spermine concentrations above $5.2 \mu\text{M}$, all individual chains are in the compact state (*c*). The integration of fluorescence signals confirms that each compact object is composed of one single chain. For intermediate spermine concentrations, $4.5 \mu\text{M} < [\text{SPM}^{4+}] < 5.2 \mu\text{M}$, chains in the elongated coil and compact states coexist (*b*), and the fraction of chains in the compact state increases with an increase in $[\text{SPM}^{4+}]$. The largely discrete nature of the conformational change and the coexistence region at intermediate spermine concentrations are the signature of the first-order nature of the single-chain folding transition of giant DNA (Yoshikawa and Matsuzawa, 1995; Yoshikawa et al., 1996).

Unfolding transition with an increase in ϵ_r

Using single-chain fluorescent microscopy, we then studied the effect of increasing ϵ_r on the DNA single-chain conformation in the presence of spermine. For very low spermine concentrations, $[\text{SPM}^{4+}] < 4.5 \mu\text{M}$, i.e., DNA in the coil state at $\epsilon_r = 80$, there was no change in conformation with an increase in ϵ_r . Conversely, at a constant spermine concentration $> 5.2 \mu\text{M}$, i.e., DNA in the compact state at $\epsilon_r = 80$, we systematically observed that DNA chains unfold with an increase in ϵ_r in a largely discrete manner at the level of single chains, as illustrated by Fig. 4. In this figure, the spermine concentration is fixed at $20 \mu\text{M}$. In water at $\epsilon_r = 80$, which corresponds to panel *c* in Figs. 3 and 4, all chains are in the compact state. When ϵ_r is increased, all chains remain in the compact state as long as $\epsilon_r < 98$. With a further

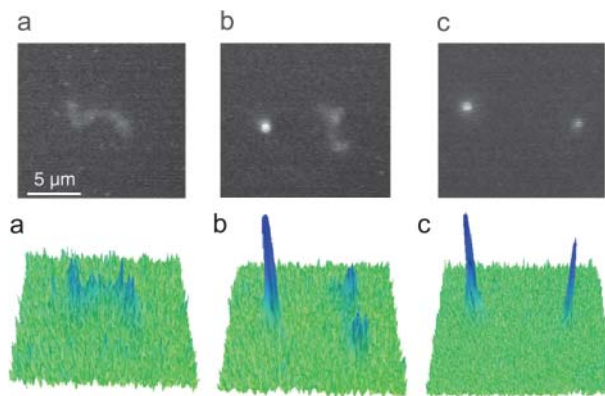


FIGURE 3 Fluorescent images (*top*) and quasi-three-dimensional representations (*bottom*) of the first-order folding transition of individual DNA chains ($0.1 \mu\text{M}$) in water ($\epsilon_r = 80$) upon the addition of spermine: (*a*) coil state at $[\text{SPM}^{4+}] = 1.5 \mu\text{M}$, (*b*) coexistence of coil and compact states at $[\text{SPM}^{4+}] = 4.9 \mu\text{M}$, and (*c*) compact state at $[\text{SPM}^{4+}] = 20 \mu\text{M}$.

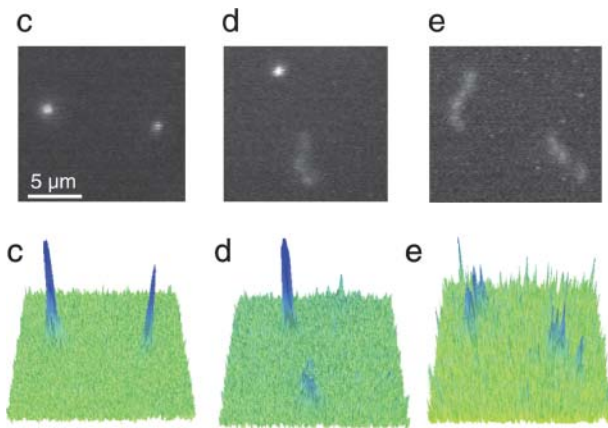


FIGURE 4 Fluorescent images (*top*) and quasi-three-dimensional representations (*bottom*) of the first-order unfolding transition of individual DNA chains at a constant spermine concentration $[SPM^{4+}] = 20 \mu\text{M}$ with an increase in the relative dielectric constant (i.e., decrease in counterion condensation): (c) compact state at $\epsilon_r = 80$, (d) coexistence of coil and compact states at $\epsilon_r = 100.8$, and (e) coil state at $\epsilon_r = 120$.

increase in ϵ_r , chains individually unfold in a largely discrete manner. At $\epsilon_r > 101.5$, all chains are in the elongated coil state (Fig. 4, *panel e*), with a typical long-axis length of $4.4 \mu\text{m}$ (see Fig. 1). For intermediate dielectric constants, $98 < \epsilon_r < 101.5$, the compact and elongated coil states coexist (Fig. 4, *panel d*), and the proportion of chains in coil state increases with an increase in ϵ_r . These features are typical of a first-order phase transition at the level of single chains. It is important to note that this first-order unfolding transition was observed over a wide range of spermine concentrations: from $8 \mu\text{M}$ to 7mM . Regardless of $[SPM^{4+}]$, the unfolding transition is always largely discrete at the level of single chains, and the critical dielectric constant at which the transition occurs increases with an increase in $[SPM^{4+}]$. To our knowledge, these results constitute the first evidence of the largely discrete unfolding transition of individual DNA chains with an increase in ϵ_r .

Folding transition as a function of ϵ_r

We then systematically studied the effect of ϵ_r on the folding transition of DNA induced by spermine. For this purpose, again using fluorescence microscopy, we characterized the conformation of single chains upon the addition of spermine at various dielectric constants. Regardless of ϵ_r , single chains undergo a first-order folding transition between the elongated coil state and the compact state in response to the addition of a sufficient amount of spermine. This transition shows the same features as that observed in pure water (see Fig. 3). The only difference is the critical spermine concentration $[SPM^{4+}]^{\text{crit}}$ at which the transition occurs. The phase diagram in Fig. 5 summarizes the experimental observations. In this graph, the critical spermine concentration at which the compact state first appears is represented by blue points, and

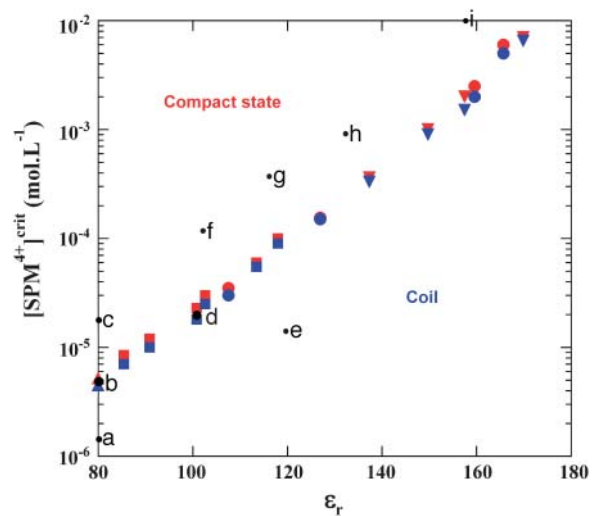


FIGURE 5 Phase diagram of individual DNA chains ($0.1 \mu\text{M}$): critical spermine concentration $[SPM^{4+}]^{\text{crit}}$ as a function of the relative dielectric constant (semilogarithmic plot). Blue symbols correspond to the appearance of the first compact states and red symbols show the disappearance of the last coils. Different symbol shapes correspond to the zwitterionic species used for ϵ_r enhancement: no zwitterion (\blacktriangle), glycine (\blacksquare), 4-aminopropanoic acid (\bullet), and 6-aminohexanoic acid (\blacktriangledown). Black points labeled from *a* to *i* correspond to the experimental conditions for the microscopic pictures presented in Figs. 3, 4, 6, and 7.

red points show when the last coils disappear. Hence, the phase diagram is divided into three zones. The coiled state is observed below the border formed by blue points and the region above the red points corresponds to the compact state. In the intervening region the two phases, i.e., coil and compact states, coexist. Fig. 5 shows that the critical spermine concentration at which the folding transition occurs is a strong increasing function of ϵ_r . Moreover, this function is independent of the chemical nature of the zwitterion used for ϵ_r enhancement. This means that the retardation of the DNA folding transition observed in these experiments is entirely due to the increase in ϵ_r and is not related to any specific chemical interaction between a particular zwitterion and the DNA chain. As shown in Fig. 5, this strong dependence of $[SPM^{4+}]^{\text{crit}}$ was noted over a range of spermine concentrations that spanned four orders of magnitude; within the limits of our experimental accuracy, $[SPM^{4+}]^{\text{crit}}$ increases exponentially as a function of ϵ_r according to the following relationship (first appearance of the compact state; *blue points* in Fig. 5):

$$[SPM^{4+}]^{\text{crit}} \propto \exp\left(\frac{\epsilon_r}{12.7}\right). \quad (3)$$

Let us summarize our experimental observations. We studied the effect of decreasing counterion condensation caused by an increasing dielectric constant on the single-chain folding transition of DNA. The properties of DNA in the coil state are almost independent of ϵ_r . Conversely, the

appearance or disappearance of the coil state, which is related to monomer-monomer “like-charged” attraction, is very sensitive to ϵ_r : i), at a fixed spermine concentration, single DNA chains unfold in a first-order manner upon an increase in ϵ_r ; and ii), at a fixed dielectric constant, DNA chains undergo a first-order folding transition upon the addition of spermine, and the critical concentration of spermine necessary to induce this transition is a strong increasing function of ϵ_r . This demonstrates the crucial importance of counterion condensation in the like-charged attraction process of the DNA single-chain folding transition. Therefore, it seems essential that we more precisely characterize the effect of ϵ_r on the like-charged state, i.e., the compact state of individual DNA chains. For this purpose, we used TEM to characterize the compact state of DNA as a function of increasing ϵ_r .

TEM of compact DNA as a function of ϵ_r

These experiments were performed at a DNA concentration of $1 \mu\text{M}$, which facilitates single-molecule detection, whereas fluorescence microscopy was performed using $0.1 \mu\text{M}$ solutions. Moreover, as mentioned in the section Coil state, the single-chain properties of T4 DNA are independent of concentration for a DNA concentration lower than $10 \mu\text{M}$ (Iwataki et al., 2004). Therefore, concentration effects can be neglected and the DNA solution considered dilute (no interaction between individual chains). In particular, the single-chain phase diagram shown in Fig. 5 is still valid under the experimental conditions for these TEM observations. Fig. 6 shows a series of typical TEM pictures of single DNA chains in the compact state for various dielectric constants. In pure water at $\epsilon_r = 80$ and $[\text{SPM}^{4+}] = 20 \mu\text{M}$, all chains are compacted into a highly ordered toroidal morphology (picture *c*) with an average outer diameter of $90 \pm 10 \text{ nm}$, in agreement with classical observations (Gosule and Schellman, 1976; Hud and Downing, 2001). Pictures *f–h* show typical morphologies observed for higher ϵ_r : 103, 115, and 131, respectively. For each dielectric constant, the spermine concentration was chosen so that the corresponding compact state is in the same relative position in the phase diagram with respect to the transition point (see *black points* labeled *c*, *f*, *g*, and *h* in Fig. 5). Indeed, it is known that at a fixed dielectric constant, a large increase in the concentration of the condensing agent can induce a swelling of the

compact toroidal state before complete unfolding (Yoshikawa et al., 1999). By comparing points in the same relative position, we can focus solely on the effect of ϵ_r , regardless of the concentration of spermine. First, we observed that, for all dielectric constants, chains are compacted in a toroidal conformation (pictures *f–h*), as observed in pure water (picture *c*). Furthermore, within the limits of our experimental accuracy, we found that the average outer diameter was independent of ϵ_r and equaled $90 \pm 10 \text{ nm}$. However, it is interesting to note that the highly ordered toroidal structure is progressively destabilized with an increase in ϵ_r . At $\epsilon_r = 103$, the toroidal morphology is very similar to that observed in water; at $\epsilon_r = 115$, the edge of the toroid becomes fuzzy, and at $\epsilon_r = 131$, small parts of the chain that are locally in the coil state form loops surrounding the toroid (arrow in picture *h*). At a much higher dielectric constant, only disordered and loosely packed structures were observed. An example of such a structure is shown in Fig. 7, for $\epsilon_r = 157$ and $[\text{SPM}^{4+}] = 10 \text{ mM}$ (point *i* in Fig. 5). In this case, a very loose toroid-like structure (indicated by arrow 1) coexists with bundles (arrow 2) and parts of the chain that are locally in the coil state (arrow 3). In summary, Figs. 6 and 7 show that the compact state becomes less ordered with an increase in the dielectric constant.

DISCUSSION

It has been shown that the presence of zwitterionic species strongly affects the single-chain DNA compaction by tetravalent spermine SPM^{4+} . Zwitterions have been dissolved in water to vary the dielectric constant in a large range ($\epsilon_r = 80\text{--}180$) while keeping constant the solvent quality. Although the dielectric constant seems to be the main parameter that controls the DNA compaction properties, one should discuss the eventual effects of the specific interaction between zwitterions and DNA. Recently, Hong et al. (2004) have shown that glycine betaine is strongly excluded from the DNA surface and that the DNA chain is preferentially hydrated. The local dielectric constant around the chain is thus expected to be different from that in the bulk solution. In the case of alcohols, Hultgren and Rau (2004) have also shown that such exclusion mechanisms can affect the DNA precipitation by multivalent counterions such as spermidine. Similarly to glycine betaine, the distribution of the zwitterions used in this study around DNA is probably not

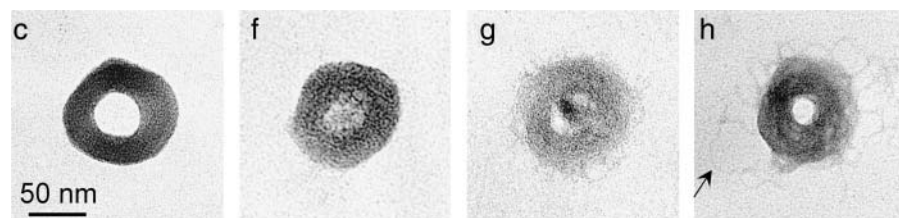


FIGURE 6 TEM pictures ($50,000\times$ magnification) of typical toroidal structures of a single DNA chain in the compact state, as a function of increasing dielectric constant: $\epsilon_r = 80, 103, 115,$ and 131 (from left to right). The spermine concentration is $20 \mu\text{M}, 100 \mu\text{M}, 300 \mu\text{M},$ and 1 mM , respectively. All pictures are shown at the same scale. The arrow in *h* indicates a loop of chain that is locally in the coil state surrounding the main toroidal structure.

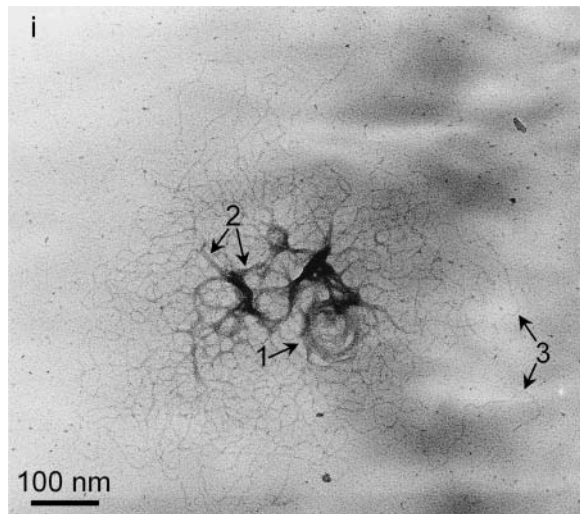


FIGURE 7 Example of a disordered and loosely packed compact state at a very high dielectric constant, as observed by TEM (50,000 \times magnification); $\epsilon_r = 157$, $[\text{SPM}^{4+}] = 10 \text{ mM}$. Arrows indicate 1), a loose toroid-like structure, 2), bundles, and 3), parts of chain that are locally in the coil state.

homogeneous, and exclusion from the DNA chain may be expected. Thus, different amplitudes in the exclusion mechanism as a function of zwitterion size and concentration could qualitatively explain the increase in $[\text{SPM}^{4+}]^{\text{crit}}$ shown in Fig. 5. However, by the use of various solvent mixtures with dielectric constants smaller than that of water, Mel'nikov et al. (1999) have shown that the dielectric constant of the solvent is the key factor that determines the conformational behavior of single DNA molecules in solution. Moreover, the effect of the dielectric constant shown in their study is in quantitatively good agreement with the results of this work (Figs. 3–5). Therefore, even if preferential hydration may be an important factor in the conformational properties of DNA, we will focus in the discussion below on the effects of the dielectric constant.

First of all, it has become clear that DNA in the compact state unfolds in a largely discrete manner at the level of single chains with an increase in ϵ_r (Fig. 4). This directly illustrates the role of counterion condensation in the DNA folding transition and, more generally, in like-charged attraction phenomena. Indeed, with all other parameters constant, an increase in ϵ_r corresponds to a decrease in counterion condensation (electrostatic energy weakens, whereas the translational entropy of counterions is constant). The unfolded coil state (like-charged repulsion) is preferred at low counterion condensation (high ϵ_r) and the compact state (like-charged attraction) is only observed at sufficiently high counterion condensation (low ϵ_r). We also noted that at fixed dielectric constant, individual DNA chains fold in a first-order manner with an increase in the spermine concentration (Fig. 3), but the critical spermine concentration $[\text{SPM}^{4+}]^{\text{crit}}$ at which the transition occurs is a strong increasing function

of ϵ_r (Fig. 5). To correlate this increase with counterion condensation, we estimated the fraction θ of the DNA charges neutralized by the counterions of valencies $Z_1 = 1$ (mainly coming from the buffer solution) and $Z_2 = 4$ (tetravalent spermine), respectively. In the two-state model of Manning-Oosawa, a fraction of these counterions, θ_1 and θ_2 respectively, are “bound” to the chain to decrease the linear charge density of the chain, whereas the other fraction remains free in the solution. Minimization of the free energy with respect to θ_1 and θ_2 leads to the following system of equations (Manning, 1978; Wilson and Bloomfield, 1979):

$$1 + \ln \frac{10^3 \theta_1}{c_1 v_1} = -2Z_1 \xi (1 - Z_1 \theta_1 - Z_2 \theta_2) \ln(1 - \exp(-\kappa b)) \quad (4)$$

$$1 + \ln \frac{10^3 \theta_2}{c_2 v_2} = -2Z_2 \xi (1 - Z_1 \theta_1 - Z_2 \theta_2) \ln(1 - \exp(-\kappa b)), \quad (5)$$

where c_1 and c_2 are the total concentration of monovalent and tetravalent counterions respectively, v_1 and v_2 are the volumes where they are assumed to be bound, ξ is the adimensional Manning parameter (l_B/b), and κ^{-1} is the Debye length. The system was solved numerically by taking for v_1 and v_2 their limiting values (infinite dilution) and the total neutralization was calculated as

$$\theta = Z_1 \theta_1 + Z_2 \theta_2. \quad (6)$$

The total neutralization θ was calculated at the onset of the folding transition (*blue points* in Fig. 5) and is plotted as a function of ϵ_r in Fig. 8. It shows that the total neutralization is remarkably constant at the onset of the transition and equals ~ 0.875 for all dielectric constants in the range 80–170, independent of the zwitterion species used for ϵ_r enhancement. This confirms the original observation of Wilson

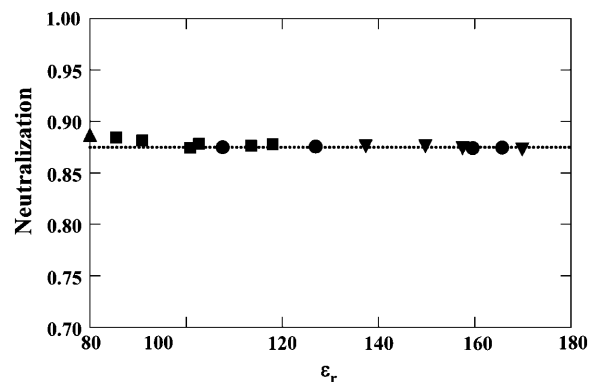


FIGURE 8 Total neutralization of DNA calculated from Eqs. 1–3 at the onset of the single-chain folding transition. Symbols correspond to blue symbols in Fig. 5 and show the zwitterionic species used for ϵ_r enhancement: no zwitterion (\blacktriangle), glycine (\blacksquare), 4-aminopropanoic acid (\bullet), and 6-aminohexanoic acid (\blacktriangledown). The horizontal dashed line indicates the average value of 0.875.

and Bloomfield (1979) that the onset of the folding transition depends only on the total charge neutralization of the DNA chain, which is mainly governed by counterion condensation. However, it is important to note that the Manning-Oosawa theory is only applicable when all DNA chains are in the coil state. This means that the above calculation is only valid for the coil state and, in the extreme limit, at the onset of the folding transition. Although the Manning-Oosawa theory describes remarkably well when the transition is initiated, it is thus inappropriate to explain the mechanism of the folding transition. This is clearly shown by the fact that chains in the coil state can coexist with chains in the compact state, where full neutralization is almost reached (e.g., *panel b* in Fig. 3). Hence, previous studies have shown that the mechanism of the folding transition is mostly driven by ion exchange between condensed monovalent and free multivalent counterions (Murayama and Yoshikawa, 1999). Thus, the difference in free energy between the coil (G_{Coil}) and folded (G_{Folded}) states depends on the chemical potential of free multivalent counterions, here spermine, abbreviated $[\text{SPM}^{4+}]_{\text{free}}$, and can be expressed as follows:

$$\Delta G_{\text{F/C}} = G_{\text{Coil}} - G_{\text{Folded}} = a \ln[\text{SPM}^{4+}]_{\text{free}} + b, \quad (7)$$

where a and b are physicochemical parameters. On the other hand, we have also observed that, at a constant spermine concentration, individual DNA chains unfold in a first-order manner when ϵ_r is increased. To estimate the dependence of $\Delta G_{\text{F/C}}$ on ϵ_r , we measured, in our fluorescence microscopic observations, the ratio of the relative population of compact (P_{F}) and coil (P_{C}) states ($P_{\text{F}}/P_{\text{C}}$) in the region of coexistence as a function of ϵ_r . Fig. 9 shows $\ln(P_{\text{F}}/P_{\text{C}})$ as a function of ϵ_r for a constant spermine concentration of 20 μM (i.e., conditions in Fig. 4). This graph confirms that the compact state is preferred at low dielectric constant and shows that,

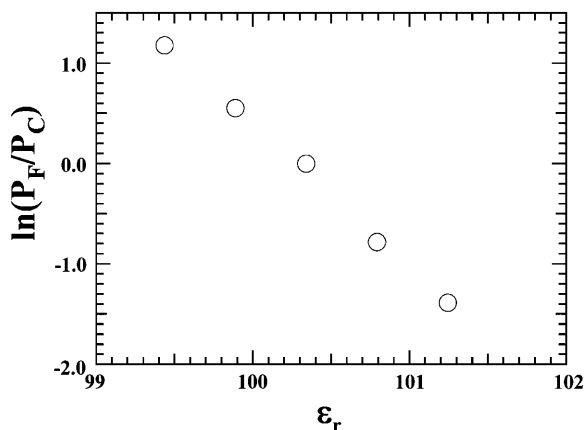


FIGURE 9 Logarithm of the ratio of relative populations of the compact state (P_{F}) and coil state (P_{C}) as a function of the relative dielectric constant ϵ_r , for a constant spermine concentration of 20 μM . Error bars are comparable to the symbol size.

within experimental error, $\ln(P_{\text{F}}/P_{\text{C}})$ depends linearly on ϵ_r . We can thus estimate $\Delta G_{\text{F/C}}$ as follows:

$$\Delta G_{\text{F/C}} = kT \ln \frac{P_{\text{F}}}{P_{\text{C}}} = -c\epsilon_r + d, \quad (8)$$

where c and d are constant parameters. From Eqs. 7 and 8, we propose the following expression for $\Delta G_{\text{F/C}}$:

$$\Delta G_{\text{F/C}} = a \ln[\text{SPM}^{4+}]_{\text{free}} - c\epsilon_r + cte. \quad (9)$$

For a given population of coil and compact states, the spermine concentration and dielectric constant are correlated as

$$\ln[\text{SPM}^{4+}]_{\text{free}} = \frac{c}{a} \epsilon + \beta, \quad (10)$$

where β is a constant that depends on the relative population of coils and globules. By extrapolating equation 10 at the onset of the folding transition, we obtain

$$\ln[\text{SPM}^{4+}]^{\text{crit}} = \frac{c}{a} \epsilon + \beta_{\text{onset}}, \quad (11)$$

which is in perfect agreement with the experimental results (Fig. 5 and Eq. 3).

Finally, the change in morphology with a change in the dielectric constant, as shown in Figs. 6 and 7, may also be of scientific value. The somewhat swollen morphology at higher dielectric constant suggests a decrease in the energy barrier between the coil and compact states. In a first-order phase transition, fluctuations are generally enhanced with a decrease in the free energy barrier. From this point of view, the highly disordered conformation presented in Fig. 7 illustrates the enhancement of fluctuations near ‘‘criticality’’.

CONCLUSION

We have studied the single-chain folding transition of giant DNA by tetravalent spermine as a function of increasing dielectric constant or decreasing counterion condensation. Changing ϵ_r had no remarkable effect on the coil state (secondary structure and characteristic size) but strongly influenced the appearance and characteristics of the compact state (like-charged attraction state). We found that at a constant spermine concentration, single chains unfold in a first-order manner with an increase in ϵ_r , which shows that the compact state is preferred at high counterion condensation. At constant ϵ_r , DNA chains fold individually (first-order phase transition) when the spermine concentration increases, but the critical concentration $[\text{SPM}^{4+}]^{\text{crit}}$ at which the transition occurs is an exponentially increasing function of ϵ_r . A rough estimation of the total DNA charge neutralization, using the Manning-Oosawa condensation theory, shows that the onset of the folding transition always occur when 87%–88% of the charges are neutralized by condensed counterions. The compact state of individual chains consists

of a toroidal structure with a diameter of ~ 90 nm, which becomes loose and less ordered with an increase in ϵ_r . These features directly illustrate the crucial role of counterion condensation in the single-chain folding transition of giant DNA, which is a typical example of a like-charged attraction phenomenon.

We gratefully acknowledge Takuya Saito, Yoshiko Takenaka, Anatoly Zinchenko, Makio Fujioka (Kyoto University), and Toshio Kanbe (Nagoya University) for experimental support and illuminating discussions.

This work was supported by the Japanese Society for Promotion of Science and by a Grant-in-Aid for the 21st Century Center of Excellence "Center for Diversity and Universality in Physics" from the Ministry of Education, Culture, Sports, Science and Technology of Japan.

REFERENCES

- Bass, S. J., W. I. Nathan, R. M. Meighan, and R. H. Cole. 1964. Dielectric properties of alkyl amides. II. Liquid dielectric constant and loss. *J. Phys. Chem.* 68:509–515.
- Bloomfield, V. A. 1996. DNA condensation. *Curr. Opin. Struct. Biol.* 6: 334–341.
- Borukhov, I., R. F. Bruinsma, W. M. Gelbart, and A. J. Liu. 2001. Elastically driven linker aggregation between two semiflexible polyelectrolytes. *Phys. Rev. Lett.* 86:2182–2185.
- Das, R., T. T. Mills, L. W. Kwok, G. S. Maskel, I. S. Millett, S. Doniach, K. D. Finkelstein, D. Herschlag, and L. Pollack. 2003. Counterion distribution around DNA probed by solution x-ray scattering. *Phys. Rev. Lett.* 90:188103.
- Deserno, M., A. Arnold, and C. Holm. 2003. Attraction and ionic correlations between charged stiff polyelectrolytes. *Macromolecules.* 36: 249–259.
- Flock, S., and C. Houssier. 1997. Effect of glycine on DNA structural transitions induced by multivalent cationic compounds. *J. Biomol. Struct. Dyn.* 15:53–61.
- Flock, S., R. Labarbe, and C. Houssier. 1995. Osmotic effectors and DNA structure. Effect of glycine on precipitation of DNA by multivalent cations. *J. Biomol. Struct. Dyn.* 13:87–102.
- Flock, S., R. Labarbe, and C. Houssier. 1996. Dielectric constant and ionic strength effects on DNA precipitation. *Biophys. J.* 70:1456–1465.
- Gosule, L. C., and J. A. Schellman. 1976. Compact form of DNA induced by spermidine. *Nature.* 259:333–335.
- Grier, D. G. 2003. Fluid dynamics: vortex rings in a constant electric field. *Nature.* 424:267–268.
- Grönbech-Jensen, N., R. J. Mashl, R. F. Bruinsma, and W. M. Gelbart. 1997. Counterion-induced attraction between rigid polyelectrolytes. *Phys. Rev. Lett.* 78:2477–2480.
- Ha, B.-Y., and A. J. Liu. 1997. Counterion-mediated attraction between two like-charged rods. *Phys. Rev. Lett.* 79:1289–1292.
- Hong, J., M. W. Capp, C. F. Anderson, R. M. Saecker, D. J. Felitsky, M. W. Anderson, and M. T. Record Jr. 2004. Preferential interactions of glycine betaine and of urea with DNA: implications for DNA hydration and for effects of these solutes on DNA stability. *Biochemistry.* 43: 14744–14758.
- Hud, N. V., and K. H. Downing. 2001. Cryoelectron microscopy of λ phage DNA condensates in vitreous ice: the fine structure of DNA toroids. *Proc. Natl. Acad. Sci. USA.* 98:14925–14930.
- Hultgren, A., and D. C. Rau. 2004. Exclusion of alcohols from spermidine-DNA assemblies: probing the physical basis of preferential hydration. *Biochemistry.* 43:8272–8280.
- Iwataki, T., S. Kidoaki, T. Sakaue, K. Yoshikawa, and S. S. Abramchuk. 2003. Competition between compaction of single chains and bundling of multiple chains in giant DNA molecules. *J. Chem. Phys.* 120:4004–4011.
- Laemmli, U. K. 1975. Characterization of DNA condensates induced by poly(ethylene oxide) and polylysine. *Proc. Natl. Acad. Sci. USA.* 72: 4288–4292.
- Lyubartsev, A. P., J. X. Tang, P. A. Janmey, and L. Nordenskiöld. 1998. Electrostatically induced polyelectrolyte association of rodlike virus particles. *Phys. Rev. Lett.* 81:5465–5468.
- Manning, G. S. 1969. Limiting laws and counterion condensation in polyelectrolyte solutions. I. Colligative properties. II. Self-diffusion of the small ions. III. An analysis based on the Mayer ionic solution theory. *J. Chem. Phys.* 51: 924–933, 934–938, 3249–3252.
- Manning, G. S. 1978. The molecular theory of polyelectrolyte solutions with applications to the electrostatic properties of polynucleotides. *Q. Rev. Biophys.* 11:179–246.
- Mel'nikov, S. M., M. O. Khan, B. Lindman, and B. Jönsson. 1999. Phase behavior of single DNA in mixed solvents. *J. Am. Chem. Soc.* 121:1130–1136.
- Mel'nikov, S. M., V. G. Sergeyev, and K. Yoshikawa. 1995. Discrete coil-globule transition of large DNA induced by cationic surfactant. *J. Am. Chem. Soc.* 117:2401–2408.
- Murayama, H., and K. Yoshikawa. 1999. Thermodynamics of the collapsing phase transition in a single duplex DNA molecule. *J. Phys. Chem. B.* 103:10517–10523.
- Odijk, T. 1977. Polyelectrolytes near the rod limit. *J. Polym. Sci.* 15:477–483.
- Olvera de la Cruz, M., L. Belloni, M. Delsanti, J. P. Dalbiez, O. Spalla, and M. Drifford. 1995. Precipitation of highly charged polyelectrolyte solutions in the presence of multivalent salts. *J. Chem. Phys.* 103: 5781–5791.
- Oosawa, F. 1971. Polyelectrolytes. Marcel Dekker, New York.
- Rouzina, I., and V. A. Bloomfield. 1996. Macroion attraction due to electrostatic correlation between screening counterions. I. Mobile surface-adsorbed ions and diffuse ion cloud. *J. Chem. Phys.* 100:9977–9989.
- Sehgal, A., and T. A. P. Seery. 1998. The ordinary-extraordinary transition revisited: a model polyelectrolyte in a highly polar organic solvent. *Macromolecules.* 31:7340–7346.
- Shklovskii, B. I. 1999. Wigner crystal model of counterion induced bundle formation of rodlike polyelectrolytes. *Phys. Rev. Lett.* 82:3268–3271.
- Skolnick, J., and M. Fixman. 1977. Electrostatic persistence length of a wormlike polyelectrolyte. *Macromolecules.* 10:944–948.
- Stevens, M. J. 1999. Bundle binding in polyelectrolyte solutions. *Phys. Rev. Lett.* 82:101–104.
- Tang, J. X., and P. A. Janmey. 1996. The polyelectrolyte nature of F-actin and the mechanism of actin bundle formation. *J. Biol. Chem.* 271:8556–8563.
- Yoshikawa, K., and Y. Matsuzawa. 1995. Discrete phase transition of giant DNA dynamics of globule formation from a single molecular chain. *Physica D.* 84:220–227.
- Yoshikawa, K., M. Takahashi, V. V. Vasilevskaya, and A. R. Khokhlov. 1996. Large discrete transition in a single DNA molecule appears continuous in the ensemble. *Phys. Rev. Lett.* 76:3029–3031.
- Yoshikawa, Y., K. Yoshikawa, and T. Kanbe. 1999. Formation of a giant toroid from long duplex DNA. *Langmuir.* 15:4085–4088.
- Yoshinaga, N., K. Yoshikawa, and S. Kidoaki. 2002. Multiscaling in a long semiflexible polymer chain in two dimensions. *J. Chem. Phys.* 116: 9926–9929.
- Widom, J., and R. L. Baldwin. 1983. Monomolecular condensation of λ -DNA induced by cobalt hexammine. *Biopolymers.* 2:1595–1620.
- Wilson, R. W., and V. A. Bloomfield. 1979. Counterion-induced condensation of deoxyribonucleic acid. A light-scattering study. *Biochemistry.* 18:2192–2196.
- Wong, G. C. L., A. Lin, J. X. Tang, Y. Li, P. A. Janmey, and C. R. Safinya. 2003. Lamellar phase of stacked two-dimensional rafts of actin filaments. *Phys. Rev. Lett.* 91:018103.